Electrochimica Acta 259 (2018) 930–938

Contents lists available at ScienceDirect

Electrochimica Acta

journal homepage: www.elsevier.com/locate/electacta

EDTA_PANI/SWCNTs nanocomposite modified electrode for electrochemical determination of copper (II), lead (II) and mercury (II) ions

Megha A. Deshmukh [a, b], Raimonda Celiesiute [c, d], Almira Ramanaviciene [d], Mahendra D. Shirsat [a], Arunas Ramanavicius [b, e, *]

[a] RUSA-Center for Advanced Sensor Technology, Department of Physics, Dr. Babasaheb Ambedkar Marathwada University, Aurangabad, 431 004, (MS) India
[b] Department of Physical Chemistry, Faculty of Chemistry and Geosciences, Vilnius University, Naugarduko St. 24, LT-03225 Vilnius, Lithuania
[c] Laboratory of Bioelectrochemistry, State Research Institute Center for Physical Sciences and Technology, Sauletekio Ave 3, LT-10257 Vilnius, Lithuania
[d] NanoTechnas – Centre of Nanotechnology and Material Science, Faculty of Chemistry and Geosciences, Vilnius University, Naugarduko St. 24, LT-03225 Vilnius, Lithuania
[e] Laboratory of Nanotechnology, State Research Institute Center for Physical Sciences and Technology, Sauletekio Ave 3, LT-10257 Vilnius, Lithuania

ARTICLE INFO

Article history:
Received 29 September 2017
Received in revised form
18 October 2017
Accepted 19 October 2017
Available online 2 November 2017

Keywords:
Polyaniline (PANI)
Single walled carbon nanotubes (SWCNTs)
Differential pulse voltammetry (DPV)
Electrochemical impedance spectroscopy (EIS)
Cyclic voltammetry
Heavy metal determination

ABSTRACT

Present investigation deals with electrochemical determination of copper(II), lead(II) and mercury(II) ions, using ethylenediaminetetraacetic acid (EDTA) chelating ligand modified polyaniline (PANI) and singe walled carbon nanotubes (SWCNTs) based nanocomposite (PANI/SWNCTs). Stainless steel (SS) electrode was modified with PANI and SWCNTs based nanocomposite. PANI/SWCNTs nanocomposite was electrochemically synthesized using potential cycling technique. Further it was modified with EDTA in the presence of 1-ethyl-3(3-(dimethylamin propyl)carbodiimide (EDC) as activating agent, using dip coating technique at room temperature. The EDTA_PANI/SWCNTs/SS electrode was characterized by cyclic voltammetry in 0.5 M H_2SO_4, which was complemented with electrochemical impedance spectroscopy (EIS). AFM and SEM analysis was applied for the morphological studies of EDTA_PANI/SWCNTs nanocomposite structure. FTIR analysis was applied for the structural and compositional analysis of EDTA_PANI/SWCNTs nanocomposite. All the characterizations were performed before and after the modification of PANI/SWCNTs nanocomposite structure with chelating ligand. Differential pulse voltammetry (DPV) was used for the determination of Cu(II), Pb(II) and Hg(II) ion concentrations. Analytical characteristic such as selectivity and sensitivity of here above-mentioned metal ions was studied. The limit of detection the EDTA_PANI/SWCNTs/SS toward Cu(II), Pb(II) and Hg(II) was determined as 0.08 μM, 1.65 μM and 0.68 μM respectively.

1. Introduction

Amongst the heavy metal ions, copper, lead, and mercury are of significant concern due to their industrial activity in some regions. Cu(II), Pb(II) and Hg(II) ions are found at high concentrations in water, soil and air. Exposure to the excess of these metal ions can result in anaemia, kidney and liver damage, gastrointestinal disorder, etc. [1–4]. Hence, there is an immense need of the effective and rapid metal ion detection; many methods are applied by research communities for metal ions monitoring including fluorescence, optics, SERS, combined methods. One of the simplest and the most rapid methods for the determination of heavy metal ion concentrations are based on electrochemistry [5–8]. The electrochemical detection of heavy metal ions plays an essential role in the selection of proper electrochemical technique and the choice of working electrode material. Most commonly used electrochemical technique for the detection of metal ions through aqueous media is anodic stripping voltammetry (ASV). Usually, this technique is based on three major steps, such as: i) analyte pre-concentration on working electrode, ii) resting step to homogenize the substance on the electrode and iii) stripping of the analyte form electrode surface [9]. The mercury electrode is more explored for heavy metal ion

* Corresponding author. Department of Physical chemistry, Faculty of Chemistry and Geosciences, Vilnius University, Naugarduko st. 24, LT-03225 Vilnius, Lithuania.
E-mail address: arunas.ramanavicius@chf.vu.lt (A. Ramanavicius).

https://doi.org/10.1016/j.electacta.2017.10.131
0013-4686/

detection; it is sensitive, reproducible and has a high cathode potential range. However, it has to be replaced with more environmentally friendly electrode material due to its toxicity [10]. Bismuth, glassy carbon, gold and boron doped electrodes [11–14] are potentially used materials. Moreover, Anodic stripping voltammetry (ASV) detection of heavy metal ion has several limitations such as instability, low sensitivity and high LOD [5].

To overcome these hurdles advanced materials are investigated for the analysis of metal ions such as conducting polymers, carbon nanotubes, graphene, metal oxides, etc. [15–23]. However, there are several limitations to the individual materials performance, e.g., organic conducting polymers are slow to charge transfer, low chemical stability, unwanted change in volume due to continuous charge discharge process [24,25]. Carbon nanotubes (CNTs) are hydrophobic in nature pH of the solution also affects the surface charge of CNTs [26,27], the major disadvantage of metal oxide materials is a good performance at high temperature only [28]. Properties of graphene such as conductivity, high electron transfer rate and large surface area depends only on the synthesis process of graphene [29,30]. To overcome these limitations functionalized or composite materials are explored by many researchers for effective and simultaneous heavy metals detection, e.g., hybrid nanocomposite of graphene, multi walled carbon nanotubes (MWCNTs), SnO_2, polymers, etc. [20,31–34].

There are some reports on metal ion detection by electrodes modified with conducting polymers [10,23,35,36]. However, according to our best knowledge, the detection of metal ions with a conducting polymer and carbon nanotube nanocomposite modified with chelating ligand through covalent bonding between nanocomposite and chelating ligand has been not reported. Therefore, in present research we have synthesized and characterized the EDTA_PANI/SWCNTs nanocomposite for design of electrode, suitable for the determination of metal ions. Herein, we have reported the conducting polymer polyaniline (PANI) and single walled carbon nanotubes (SWCNTs) composite modified with ethylenediaminetetraacetic acid (EDTA) for the simultaneous and ultrasensitive detection of Cu, Pb and Hg. The PANI/SWCNTs nanocomposite have the π-π interaction, which overcomes the limitations of individual materials [16]. In the composite formation, SWCNTs acted as conducting backbone of the structure wrapping with PANI, so it can tackle the hydrophobic nature of SWCNTs. The π-π interaction between SWCNTs and PANI exceeds the charge transfer ratio of PANI which help for faster signal transduction and increase the sensitivity of the sensor [16]. Further, modification of nanocomposite structure by EDTA resolves the problem of selectivity; EDTA has the ring like structure which helps to bind with a particular metal ion from aqueous medium. These advantages of EDTA modified PANI/SWCNTs structure makes a promising sensing electrode suitable for the electrochemical detection of Cu(II), Pb(II) and Hg(II) metal ions.

Differential pulse voltammetry (DPV) technique was used for the analysis, which can overcome multistep analysis such as anodic stripping voltammetry (ASV). DPV technique is an ideal technique for the determination of heavy metal ions.

The aim of this research was to improve DPV based determination of Cu(II), Pb(II) and Hg(II) ion concentrations by polyaniline (PANI), single walled carbon nanotubes (SWCNTs), and ethylenediaminetetraacetic acid (EDTA) modified stainless steel electrode.

2. Experimental

2.1. Materials and reagents

Aniline of reagent grade was purchased from Fluka (Germany), dodecyl benzene sulphonic acid sodium salt (DBSA) of purified grade was obtained from Kemphasol (Bombay, India) and used as the surfactant and an organic solvent to form a fine suspension of SWCNTs, SWCNTs were purchased from Nanoshel LLC (USA). Ethylenediaminetetraacetic acid (EDTA) was purchased from Fisher Scientific (USA), 1-ethyl-3-(3-dimethylamin propyl) carbodiimide hydrochloride (EDC) was procured from Sigma Aldrich (Germany), sulphuric acid, phosphate buffer, pH 7, and other chemicals were of reagent grade quality and were used as received. Stainless Steel (SS) type 304, 0.5 mm thick and geometrical surface area 1×1 cm^2 was purchased from SSD Enterprises (Aurangabad, India). An acetate buffer solution was prepared by adjusting 0.2 M sodium acetate (Aldrich) to the desired pH with the addition of 0.2 M glacial acetic acid. All the processes that performed in aqueous media and the preparation of the aqueous solutions were carried out using ultrapure quality of water.

2.2. Apparatus

Differential pulse voltammetry (DPV), cyclic voltammetry (CV) and electrochemical impedance spectroscopy (EIS) were performed with potentiostat/galvanostat Autolab PGSTAT128N controlled by NOVA 1.10 software, both from ECO-Chemie (Utrecht, The Netherlands). All electrochemical measurements were carried out in three electrode cell system, whereas SS or modified SS was used as a working electrode, $Ag/AgCl_{(3M\ KCl)}$ as a reference electrode and platinum wire as a counter electrode. FTIR measurements for the confirmation of chemical composition of PANI/SWCNTs and EDTA_PANI/SWCNTs nanocomposites were carried out using FTIR-ATR spectrophotometer Frontier from Perkin Elmer (Waltham, USA). Tapping-mode atomic force microscopy (Park AFM, South Korea) and scanning electron microscopy (SEM SU70) was performed to examine the surface morphology of PANI/SWCNTs nanocomposite and EDTA_PANI/SWCNTs nanocomposite structure deposited on SS substrate.

2.3. Preparation of PANI/SWCNTs nanocomposite

A suspension of 20% of SWCNTs with respect to 0.25 M of aniline monomer was obtained by sonication with DBSA in 1 mL ultra-pure water for 4 h until suspension become stable. SDBS was used as a surfactant; the ratio of SWCNTs to surfactant was 1:10. Afterwards, 100 mL of aqueous 0.25 M aniline and 0.5 M H_2SO_4 solution was prepared with continuous stirring for 20 min. Before and after the addition of prepared SWCNTs suspension to the electrolyte it was stirred again for 20 min. The resulting suspension was used for the synthesis of the nanocomposite structure.

The cyclic voltammetry technique was used for the electrochemical synthesis of PANI/SWCNTs nanocomposite structure. The potential was swept for 20 times in cyclic manner between 0.1 and 1.0 V at the sweep rate of 0.1 V/s. The nanocomposite layer formation on working electrode was observed by the formation of dark green colored coating, the intensity of coating color increased by number of the applied potential cycles. The deposited dark green colored film was washed thoroughly with deionized water to remove the excess of aniline monomer on a substrate surface, and further it was dried at room temperature. The obtained electrode further indicated as PANI/SWCNTs/SS. A scheme of SS surface modification by PANI/SWCNTs nanocomposite and further modification of PANI/SWCNTs nanocomposite with EDTA chelating ligand is depicted in Fig. 1.

2.4. Modification of PANI/SWCNTs composite

There are several major ways for the functionalization of

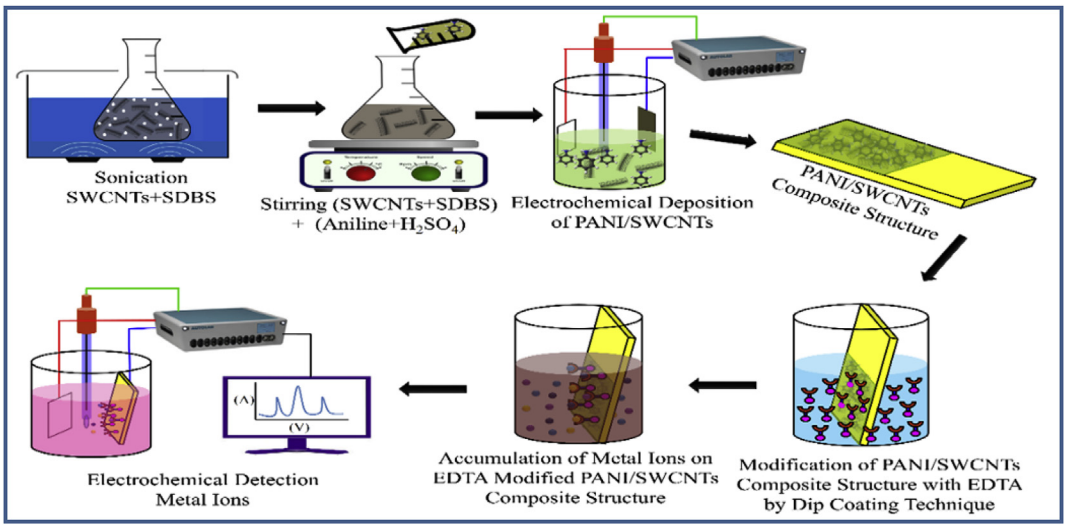

Fig. 1. Schematic for the formation of EDTA_PANI/SWCNTs nanostructure on SS electrode and further application of EDTA_PANI/SWCNTs/SS electrode the determination of heavy metal ions by DPV technique.

conducting polymers mostly performed before, during, and after formation of conducting polymer layer on the surface of electrode. In this work, we have applied the functionalization of PANI/SWCNTs nanocomposite layer by EDTA after deposition of this layer on the SS-based electrode. This way is suitable for the functionalization of formed PANI/SWCNTs nanocomposite layer, because after the polymerization another active groups can be covalently attached to the conducting polymer [37]. EDTA solution was prepared in a 0.2 M phosphate buffer solution of pH 7.2, containing 0.1 M EDC (as an activating agent) and 0.01 M EDTA. PANI/SWCNTs/SS electrodes were immersed in the prepared solution of EDTA for 12 h with continuous stirring at room temperature. The resulting EDTA_PANI/SWCNTs/SS electrodes were washed thoroughly with deionized water to remove the loosely bound molecules. In such way modified electrodes are further indicated as EDTA_PANI/SWCNTs/SS.

2.5. Electrochemical detection of metal ions

The electrochemical detection of Cu(II), Pb(II) and Hg(II) ions accomplished in a system containing a three-electrode setup at room temperature. Herein, the EDTA_PANI/SWCNTs/SS electrode with geometric area of 1 cm^2 was applied as the working electrode, $Ag/AgCl_{(3M\ KCl)}$ as the reference electrode and a platinum wire as counter electrode, 0.5 M H_2SO_4 solution was used as the electrolyte for stripping of the metal ions. For differential pulse voltammetry (DPV) test, EDTA_PANI/SWCNTs/SS was immersed into the electrolyte containing from 2 mM to 1.2 μM, from 37 μM to 2 μM and from 2 mM to 2 μM of Cu(II), Pb(II) and Hg(II) ions in 0.2 M acetate buffer solution of pH 4.5, 4.9 and 4.1, respectively for complex formation of each metal ion with EDTA_PANI/SWCNTs/SS. EDTA is a multidentate ligand having ability of forming complex with many metal ions in different pHs. For the determination of EDTA_PANI/SWCNTs/SS electrode selectivity towards Cu(II), Pb(II) and Hg(II) ions, within an analyte solution containing 2 mM of Co(II), 2 mM of Ni(II) and 2 mM of Cd(II) metal ions were added. After pre-accumulation of metal ions on the electrode at room temperature, followed by a DPV scan toward positive potential (with a step increment of 5 mV, the step amplitude of 50 mV and a pulse period of 0.2 s) at the potential range from −0.26 to +0.04 V for Cu (II) ions, at −0.54 to −0.40 V for Pb (II) ions and at 0.0 to +0.3 for Hg (II) metal ions stripping from working electrode was followed. The whole experimental setup is depicted in Fig. 1.

3. Results and discussion

3.1. Electrochemical formation of PANI/SWCNTs nanocomposite

PANI/SWCNTs nanocomposite film was synthesized using potential cycling as it is described in Section 2.3 from the SWCNTs and aniline monomer suspended in 0.5 M H_2SO_4 electrolyte. Fig. 2 illustrates the typical cyclic voltammograms, which were registered during the formation of PANI/SWCNTs nanocomposite structure. 20 potential cycles from 0.1 to 1.0 V at the sweep rate of 100 mV/s were applied. During synthesis, dark green colored coating of PANI/SWCNTs nanocomposite was formed on the SS electrode. Peaks A-C in Fig. 2 corresponds to the formation of radical-cations (peak A at 0.3 V), oxidation of head to tail dimmer (peak B at 0.6 V) and conversion of PANI emeraldine form to pernigraniline structure form (peak C at 0.9 V) [34]. Conductivity of the film is increased by the number of applied potential cycles, this corresponds to the regular growth of composite structure onto the SS substrate [38]. The π-π interaction between PANI and SWCNTs [16,18,39] is

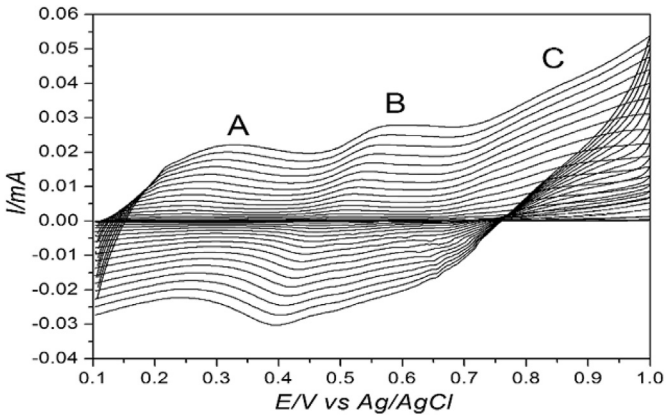

Fig. 2. Cyclic voltammograms recorded during the synthesis of PANI/SWCNTs nanocomposite structure on SS electrode. 20 potential cycles at potential scan rate of 100 mV s^{-1} in 0.5 M H_2SO_4 with 0.25 M of aniline in presence of SWCNTs were applied.

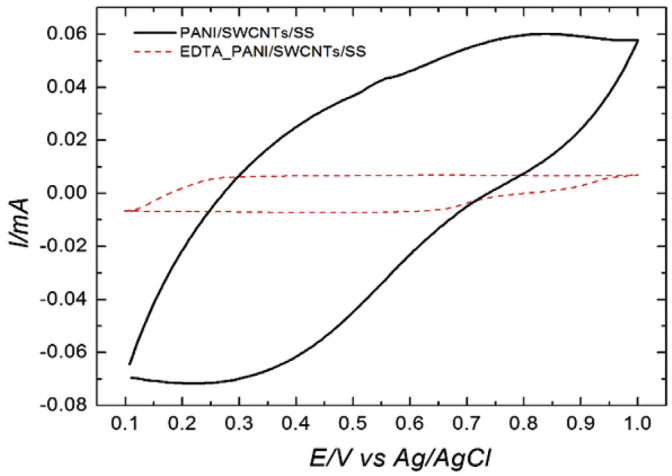

Fig. 3. CVs of PANI/SWCNTs/SS (solid line) and EDTA_PANI/SWCNTs/SS (dotted line) electrodes in 0.5 M H_2SO_4 at the scan rate of 100 mV s^{-1}.

responsible for increasing the conductivity of resulting composite structure [15,40–43].

3.2. Electrochemical characterization of EDTA_PANI/SWCNTs/SS electrode

The incorporation of EDTA within PANI/SWCNTs nanocomposite structure was confirmed by CV and EIS. The difference of CVs recorded for both (i) PANI/SWCNTs/SS and (ii) EDTA_PANI/SWCNTs/SS electrodes are shown in Fig. 3: CV of the unmodified PANI/SWCNTs/SS electrode shows higher currents, which is characteristic for larger double layer capacity as compared to EDTA_PANI/SWCNTs/SS electrode. This is due to the influence of dielectric layer of EDTA formed on interface of PANI/SWCNTs nanocomposite.

The PANI/SWCNTs/SS and EDTA_PANI/SWCNTs/SS electrodes were characterized by EIS, which is an effective tool for detailed evaluation of processes, which are taking place at electrode surfaces [44]. Fig. 4 represents the EIS Nyquist plots of PANI/SWCNTs/SS and EDTA_PANI/SWCNTs/SS electrodes. For EIS measurements working electrode potential of 0 V *vs* Ag/AgCl was applied and EIS spectra was recorded in frequency region from 1 Hz up to 100000 Hz with amplitude 0.005 V in aqueous solution of 0.5 M H_2SO_4. EIS for EDTA_PANI/SWCNTs/SS showed relatively large semicircle domain, which infers a large interfacial electron transfer resistance between redox-probe and EDTA_PANI/SWCNTs/SS electrode. For PANI/SWCNTs/SS lower interfacial electron resistance is observed from Nyquist plots, which indicates that PANI/SWCNTs nanocomposite structure promote electron transfer ultimately indicating the very good electrochemical activity of the PANI/SWCNTs nanocomposite.

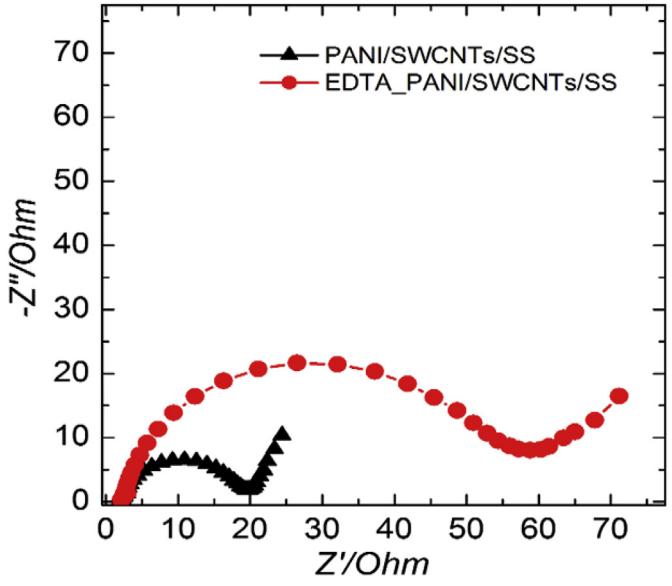

Fig. 4. EIS Nyquist plots of PANI/SWCNTs/SS and EDTA_PANI/SWCNTs/SS electrodes in 0.5 M H_2SO_4 electrolyte.

3.3. FTIR characterization of PANI/SWCNTs and EDTA_PANI/SWCNTs structure

Fig. 5 represents the FTIR spectra of both electrochemically synthesized PANI/SWCNTs and EDTA_PANI/SWCNTs nanocomposite structures. A FTIR spectrum of PANI/SWCNTs-nanocomposite has characteristic features of PANI and SWCNTs. The characteristic bands of PANI structure are observed at 802 cm^{-1}, 1070 cm^{-1}, 1290 cm^{-1}, 1496 cm^{-1}, 1560 cm^{-1}, 2932 cm^{-1}, 3209 cm^{-1} [45–47]. The presence of bands at 1478 cm^{-1}, 1594 cm^{-1} indicate presence of benzoid and quinoid bands emphasizing the formation of emeraldine salt form of PANI in the both the structures of PANI/SWCNTs and EDTA_PANI/SWCNTs nanocomposite. The band showing conducting emeraldine salt form, indicating conductive form of PANI in spectra appears at nearly 1294 cm^{-1} [48]. The band at 1294 cm^{-1} is attributed to the conducting form of the PANI, which is indicating that the PANI exists mainly in the conducting emeraldine salt form. The C=N stretching vibrations of imine group in PANI/SWNTS and EDTA_PANI/SWNTs nanocomposite were observed at 1652 cm^{-1}, while this band was suppressed in EDTA_PANI/SWNTs nanocomposite due to the presence of EDTA moieties on PANI/SWNTs nanocomposite. The C–N stretching of aromatic amine group was observed at 1237 cm^{-1} in the PANI/SWNTs and EDTA_PANI/SWTNs, respectively. The peak at 880 cm^{-1} confirms the presence of SWCNTs in the form of amorphous carbon, band around 1587 cm^{-1}, which indicates the tangential mode of SWCNTs [49]. These evidences confirm the presence of SWCNTs in PANI/SWCNTs and EDTA_PANI/SWCNTs nanocomposite structures. In addition, the C–N stretching vibrations of aromatic groups in the PANI/SWCNTs and EDTA-PANI/SWCNTs nanocomposite structures were observed at 1238 cm^{-1} and 1241 cm^{-1} respectively, which confirms presence of PANI. Band at 1730 cm^{-1} of C=O stretching in carboxylic acid of EDTA bonded structure has been observed, which was not observed in the PANI/SWNTs nanocomposite. The presence of C=O band at 1730 cm^{-1} confirms the presence of carboxylic acid indicating that EDTA moieties has covalently attached to the PANI/SWNTs nanocomposite.

3.4. Morphological characterization of PANI, PANI/SWCNTs and EDTA_PANI/SWCNTs nanocomposite structure

The morphology of PANI, PANI/SWCNTs and EDTA_PANI/SWCNTs nanocomposite structures was investigated using SEM and AFM. From Fig. 6A we can observe clusters structure of PANI thin film. Fig. 6A shows the comparatively smooth surface of bare PANI compared to the surface of PANI/SWCNTs (Fig. 6B) and EDTA_PANI/SWCNTs (Fig. 6C). Fig. 6B shows that SWCNTs are covered by electrochemically synthesized PANI structure, where SWCNTs are playing the role of the backbone of the nanocomposite. Meanwhile, the EDTA_PANI/SWCNTs nanocomposite structure displays uneven and agglomerated form of modified nanocomposite structure

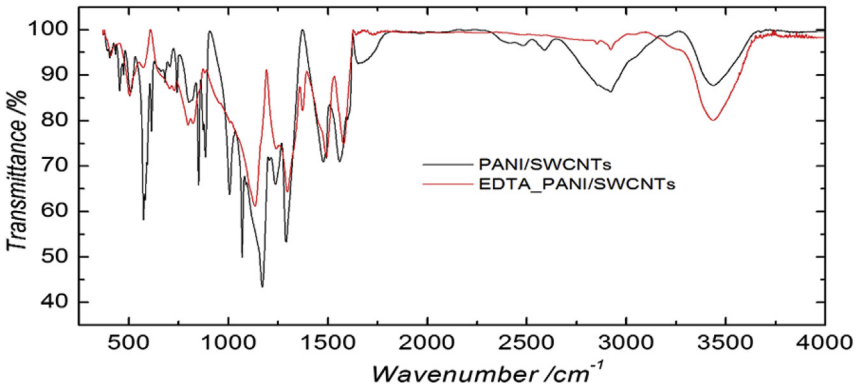

Fig. 5. FTIR spectra of (a) PANI/SWCNTs and (b) EDTA_PANI/SWCNTs nanocomposite structures.

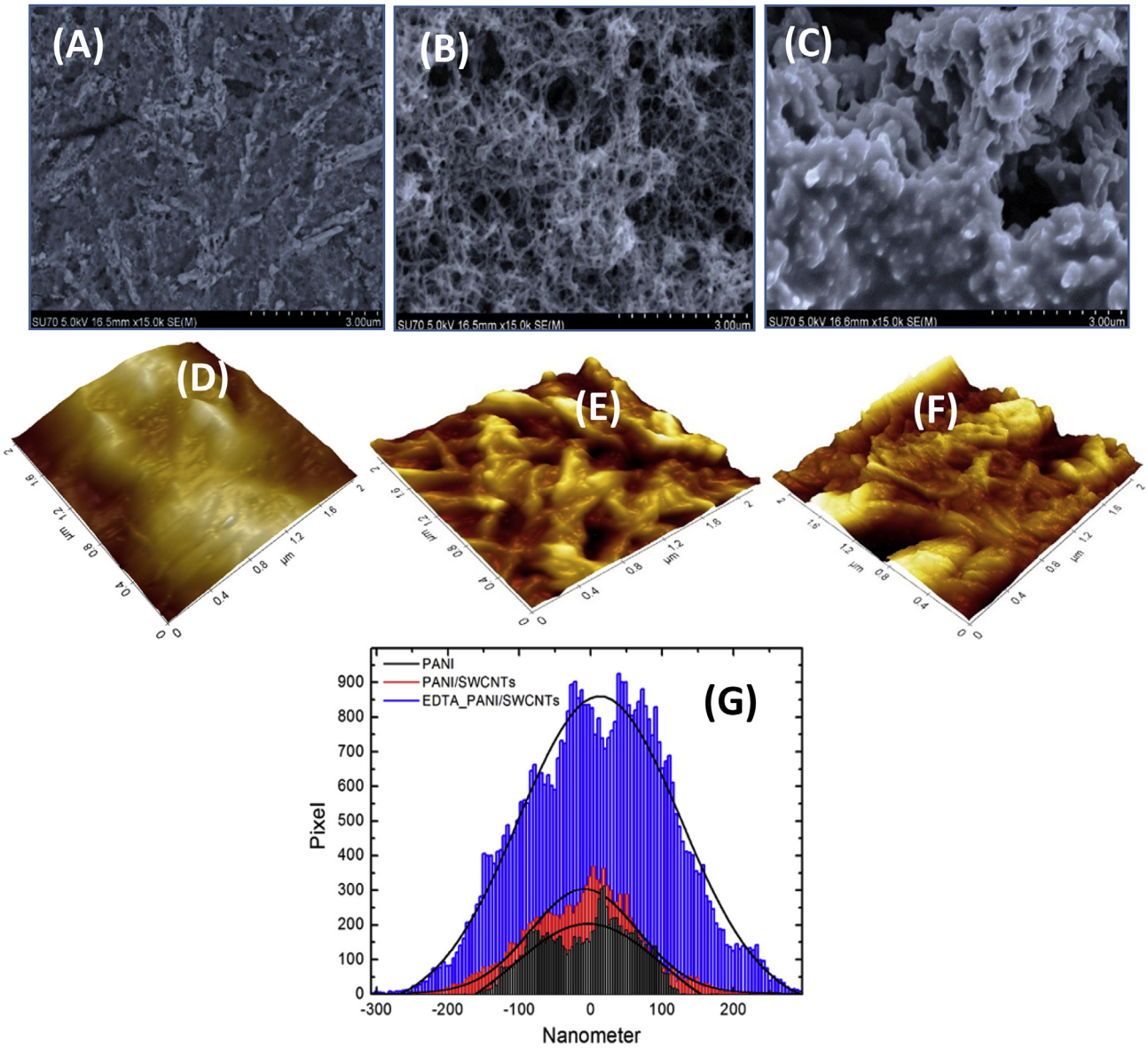

Fig. 6. SEM images of (A) PANI, (B) PANI/SWCNTs and (C) EDTA_PANI/SWCNTs nanocomposite structure, AFM images of (D) PANI, (E) PANI/SWCNTs and (F) EDTA_PANI/SWCNTs nanocomposite structure. (G) Height distribution histogram of PANI (Black region), PANI/SWCNTs (Red region) nanocomposite and EDTA_PANI/SWCNTs (Blue region) nanocomposite obtained from AFM.

(Fig. 6C). EDTA is accumulated on the surface of PANI/SWCNTs nanocomposite structure. Comparatively, a very significant structural difference can be observed in both the EDTA modified and unmodified structures, thereby demonstrating better adhesion and strong structural bonding of the EDTA to the PANI/SWCNTs nanocomposite structure during formation of EDTA_PANI/SWCNTs nanocomposite structure. The significant changes after modification of composite structure was observed, EDC was playing the role of an activating agent, responsible for the activation of carboxyl groups suitable for coupling of primary amines to vintage amide bonds. This phenomenon was responsible for activation of modified surface with drastic changes in surface morphology after the modification.

The AFM images are also revealing the same conclusion of morphological differences within bare PANI (Fig. 6D), PANI/SWCNTs (Fig. 6E) and EDTA modified PANI/SWCNTs (Fig. 6F) nanocomposite structures. The EDTA modified structure shows rougher surface compared to bare PANI and unmodified PANI/SWCNTs nanocomposite structure. Height distribution histograms (Fig. 6G) calculated for bare PANI, PANI/SWNTs nanocomposite and the EDTA modified PANI/SWNTs nanocomposite structures show significant differences. Height distribution as well as the roughness of bare PANI, PANI/SWNTs nanocomposite and EDTA_PANI/SWCNTs nanocomposite is obtained from AFM analysis. Like SEM images, AFM analysis also confirms the change in the morphology of formed layer after the modification with EDTA. The change in roughness parameter of bare PANI, PANI/SWNTs nanocomposite before and after the modification, Table 1 clearly shows that after modification there is increase in both height and roughness of the surface was observed. This evidence also reveals the presence of EDTA on the surface of PANI/SWCNTs nanocomposite structure. Advanced roughness increases effective area of the electrode, therefore, EDTA-modified structure is more beneficial for the trapping and/or accumulation of metal ions on such modified electrode surface. The presence of EDTA on EDTA_PANI/SWCNTs nanocomposite structure can significantly disturb even and rigid structure of PANI/SWCNTs nanocomposite and therefore it increases the roughness of nanocomposite structure. In addition, EDTA plays an important role in the selective complexation of metal ions, which is important for their electrochemical determination.

3.5. The determination of Cu(II), Pb(II), and Hg(II) ions

Optimal, experimental conditions for the determination of Cu(II), Pb(II) and Hg(II) ions by EDTA_PANI/SWCNTs/SS electrode using DPV technique were elaborated individually for each electrode. Accumulation of the Cu(II), Pb(II) and Hg(II) ions was carried out by incubation of the working electrode in acetate buffer solution of pH 4.5, 4.9 and 4.1 respectively, which leads to the complexation of metal ions with EDTA_PANI/SWCNTs layer. This Cu(II), Pb(II) and Hg(II) ions chemical accumulation process has advantages over the application of reduction potential, which can affect the accumulation of interfering species reducible at applied potential during pre-concentration stage. After the pre-accumulation of metal species on EDTA_PANI/SWCNTs/SS electrode, it was washed with distilled water to remove the loosely bound species from the EDTA_PANI/SWCNTs/SS electrode surface. After that the pre-accumulated EDTA_PANI/SWCNTs/SS electrode was transferred to electrochemical cell containing blank solution of 0.5 M H_2SO_4. The 0.5 M solution of H_2SO_4 was selected as an electrolyte for stripping of metal ions because the same pH used for the accumulation of metal ions at EDTA_PANI/SWCNTs/SS electrode generated noisy current response, which may be caused by the formation of hydroxide precipitates of same metal ions. The DPV response was recorded for each individual metal ion, i.e. Cu(II), Pb(II) and Hg(II).

Fig. 7 shows the DPV responses toward all evaluated heavy metal ions. Clear peaks, proportional to the concentration of Cu(II), were observed in the range from 1.2 μM to 2 mM (Fig. 7A), the limit of detection (LOD) for Cu(II) was 0.08 μM. The DPV responses towards Pb(II) and Hg(II) over a concentration ranges from 2 μM to 37 μM and 2 μM to 2 mM are shown in Fig. 7B and C, respectively. The LODs for Pb(II) and Hg(II) were 1.65 μM and 0.68 μM, respectively. The limit of detections (LODs) for each metal ion was calculated using formula:

$$LOD = 3 \times (\text{standard deviation of the regression line } (\sigma))/\text{Slope}(S)$$

Fig. 7A1, 7B1 and 7C1 represents the analytical signal at different concentrations of Cu(II), Pb(II) and Hg(II) ions, respectively. As it is seen from calculated analytical data, which are representing dependences of analytical signals on the concentration of Cu(II), Pb(II) and Hg(II) ions (Fig. 7A3, 7B3 and 7C3), they can be approximated by hyperbolic function; $y = a - b/(1 + c \times x)^{\wedge}(1/d)$ with different parameters, which are represented in Table 2 and Fig. 7A4, 7B4 and 7C4. Such approximation by hyperbolic equation is typical if concentrations of analytes are measured in very broad concentration region, while in shorter regions linear regression can be applied in order to simplify measurement/calculation of concentrations.

Subsequently, the simultaneous detection of Cu(II), Pb(II) and Hg(II) ions with the EDTA_PANI/SWCNTs/SS electrode was carried out to determine whether other cations, such as Co(II), Ni(II) and Cd(II) at 2 mM concentrations are interfering the determination of Cu(II), Pb(II) and Hg(II) ions. Fig. 8 illustrates the simultaneous and selective detection of Cu(II), Pb(II) and Hg(II) ions. DPV voltammograms of the EDTA_PANI/SWCNTs/SS after successive additions of 2 mM of Cu(II), Pb(II) and Hg(II) along with Co(II), Ni(II) and Cd(II) ions are shown in Fig. 8. The DPV voltammogram exhibits well-built and separated stripping peaks only for all Cu(II), Pb(II) and Hg(II), no significant effect was observed after the addition of 2 mM of Co(II), Ni(II) and Cd(II). The characteristic peaks of Cu(II), Pb(II) and Hg(II) were observed at −0.229, −0.481 and 0.158 V, respectively. These results are in agreement with the individual metal ion stripping characteristics (Fig. 8) with a pre-concentration time of 20 min.

Table 1
Observed roughness parameters of PANI, PANI/SWNTs and EDTA modified PANI/SWNT nanocomposite.

	PANI	PANI/SWCNTs	EDTA_PANI/SWCNTs	Parameters
Region	Whole	Whole	Whole	
Max (nm)	128.258	291.157	293.629	Maximum Roughness
Mean (nm)	−119.165	−0.163	8.86	Mean Roughness
RPv (nm)	247.473	537.7	603.228	Peak-to-Valley Roughness
Rq (nm)	51.146	78.653	100.258	Root Mean-Square Roughness
Ra (nm)	43.333	62.993	81.963	Roughness Average
Rz (nm)	238.415	515.146	595.359	Ten Point Average Roughness

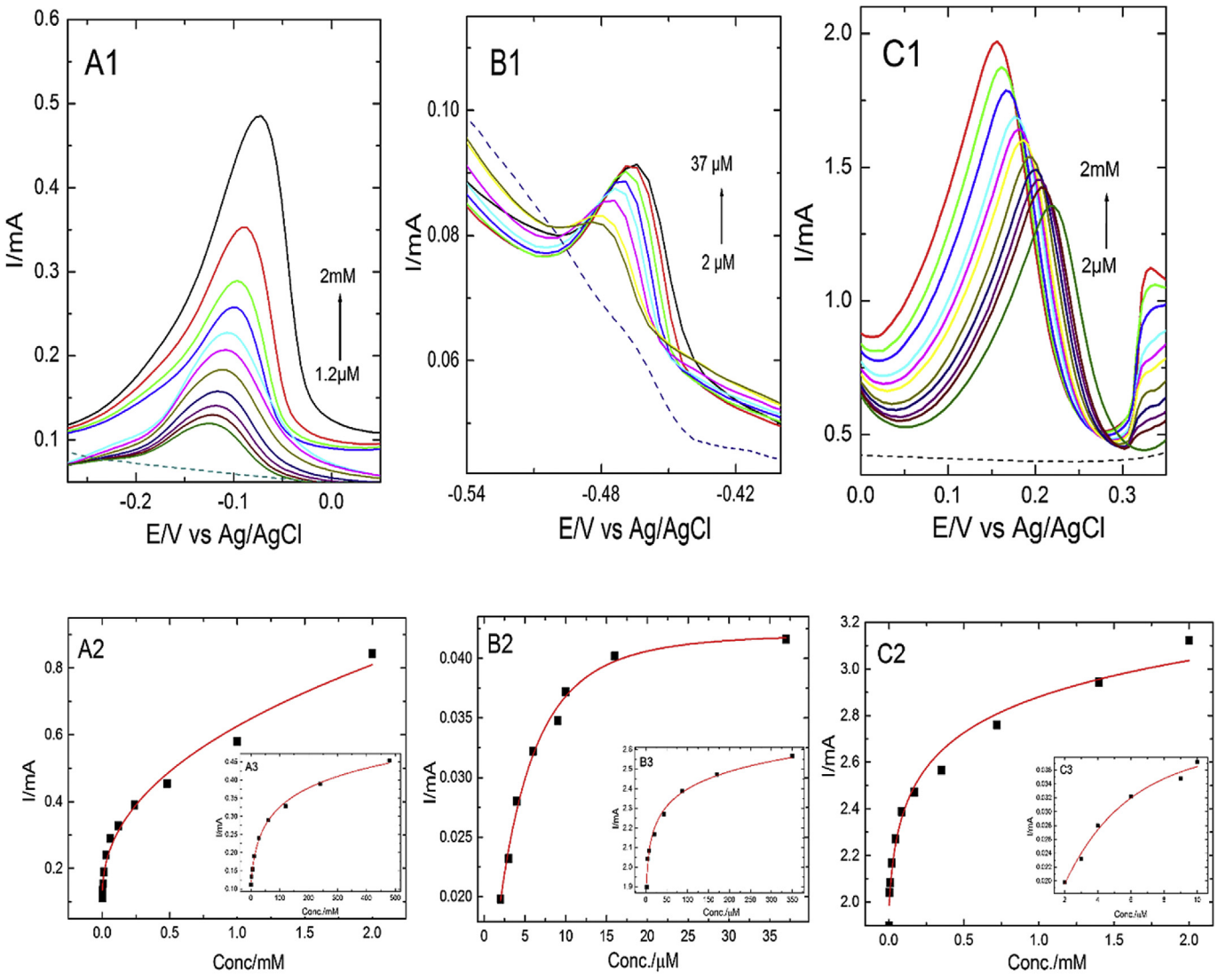

Fig. 7. DPV response of the EDTA_PANI/SWCNTs nanocomposite for the individual analysis of (A1) Cu(II) over a concentration range of 2 mM to 1.2 μM, (B1) Pb(II) over a concentration range of 37 μM to 2 μM and (C1) Hg(II) over a concentration range of 2 mM to 2 μM. A2, B2 and C2 are peak currents plotted against Cu(II), Pb(II) and Hg(II) concentrations, respectively. A3, B3 and C3 represents peak currents plotted against Cu(II). Pb (II) and Hg (II) concentrations in shorter concentration diapason approximated by hyperbolic equation $y = a - b/(1 + c \times x)^{\wedge}(1/d)$.

Table 2
A4, B4 and C4 represents corresponding parameters of applied hyperbolic equation. Supporting electrolyte, 0.5 M H_2SO_4.

Model	HyperbolaGen			Model	HyperbolaGen			Model	HyperbolaGen		
Equation	y=a−b/(1 + c*x)^(1/d)			Equation	y=a−b/(1 + c*x)^(1/d)			Equation	y=a−b/(1 + c*x)^(1/d)		
Reduced Chi-sq	3.82644E-5			Reduced Chi-sq	1.08448			Reduced Chi	9.00695		
Adj. R-Squar	0.9956			Adj. R-Squar	0.98971			Adj. R-Squar	0.98299		
		Value	Standard Error			Value	Standard Error			Value	Standard Error
A4	a	0.03021	0.06922	B4	a	0.6608	2.01252	C4	a	−0.58154	11.26592
	b	−0.02314	1.76543		b	0.617	2.1059		b	−1.56444	3761.98359
	c	248763.70	8.02317E7		c	52.243	873.59248		c	2.03287	1.09863E1
	d	−4.27569	1.19785		d	0.4402	8.32796		d	−22.5278	86.0292

4. Conclusions

Novel EDTA_PANI/SWCNTs nanocomposite was synthesized on surface of SS electrode by potential cycling and the application of the EDTA_PANI/SWCNTs/SS electrode for the detection of Cu(II), Pb(II) and Hg(II) ions was demonstrated. EDTA_PANI/SWCNTs/SS electrode is an excellent substitute for the hanging mercury drop electrode and thin mercury film electrode based electrodes, the EDTA_PANI/SWCNTs electrode exhibits much better sensitivity during the electrochemical detection of trace amounts of Cu(II), Pb(II) and Hg(II) ions, with the LODs of 0.08 μM for Cu(II), 1.65 μM for Pb(II) and 0.68 μM for Hg(II). Cu(II), Pb(II) and Hg(II) ions were determined simultaneously and selectively by means of the novel EDTA modified PANI/SWCNTs nanocomposite electrode. The

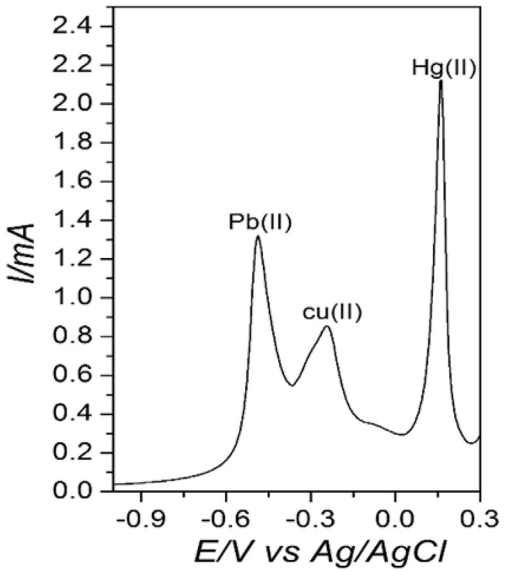

Fig. 8. DPV response of the EDTA_PANI/SWCNTs nanocomposite for the simultaneous analysis of Cu(II), Pb(II), and Hg(II) in the presence 2 mM of Co(II), 2 mM of Ni(II) and 2 mM of Cd(II).

EDTA_PANI/SWCNTs/SS-based electrode shows good selectivity towards Cu(II), Pb(II) and Hg(II) ions and can be applied for their simultaneous detection. The EDTA chelation ability and PANI/SWCNTs nanocomposite structure increases the sensitivity of EDTA_PANI/SWCNTs/SS-based electrode in comparison to that of PANI/SWCNTs/SS-based electrode.

Acknowledgement

This work was supported by the Department of Science and Technology (DST)-SERB, New Delhi, India (Project No.SB/EMEQ-042/2013), and Inter University Accelerator Center (IUAC), New Delhi, India (UFR No.55305) and "UGC-SAP, New Delhi, India (F.530/16/DRS-I/2016 (SAP-II)); Rashtriaya Uchhatar Shiksha Abhiyan, Govt. of Maharashtra, India (RUSA/order/R&I/2016-17)". Almira Ramanaviciene, Arunas Ramanavicius and Raimonda Celiesiute are are acknowledging financial support by a grant (No. S-LAT-17-1) from the Research Council of Lithuania.

References

[1] P.B. Tchounwou, C.G. Yedjou, A.K. Patlolla, Heavy metals toxicity and the environment, EXS 101 (2012) 133–164.
[2] K. Asaduzzaman, M.U. Khandaker, N.A.B. Baharudin, Y.B. Mohd Amin, M.S. Farook, D.A. Bradley, O. Mahmoud, Heavy metals in human teeth dentine: a bio-indicator of metals exposure and environmental pollution, Chemosphere 176 (2017) 221–230.
[3] S. Chowdhury, M.A.J. Mazumder, O. Al-Attas, T. Husain, Heavy metals in drinking water: occurrences, implications, and future needs in developing countries, Sci. Total Environ. 569–570 (2016) 476–488.
[4] R.A. Wuana, F.E. Okieimen, Heavy metals in contaminated soils: a review of sources, chemistry, risks and best available strategies for remediation, ISRN Ecol. 2011 (2011) 1–20.
[5] M. Li, H. Gou, I. Al-Ogaidi, N. Wu, Nanostructured sensors for detection of heavy metals: a review, ACS Sustain. Chem. Eng. 1 (2013) 713–723.
[6] D.T. Quang, J.S. Kim, Fluoro- and chromogenic chemodosimeters for heavy metal ion detection in solution and biospecimens, Chem. Rev. 110 (2010) 6280–6301.
[7] S. Wang, E.S. Forzani, N. Tao, Detection of heavy metal ions in water by high-resolution surface plasmon resonance spectroscopy combined with anodic stripping voltammetry, Anal. Chem. 79 (2007) 4427–4432.
[8] G. March, T.D. Nguyen, B. Piro, Modified electrodes used for electrochemical detection of metal ions in environmental analysis, Biosens 5 (2015) 241–275.
[9] J. Barón-Jaimez, M.R. Joya, J. Barba-Ortega, Anodic stripping voltammetry-ASV for determination of heavy metals, J. Phys. Conf. Ser. 466 (2013) 012023.
[10] J. Barek, Possibilities and limitations of mercury and mercury-based electrodes in practical electroanalysis of biologically active organic compounds, Port. Electrochim. Acta 31 (2013) 291–295.
[11] Y. Oztekin, Z. Yazicigil, A.O. Solak, Z. Ustundag, A. Okumus, Z. Kilic, A. Ramanaviciene, A. Ramanavicius, Phenanthroline derivatives electrochemically grafted to glassy carbon for Cu(II) ion detection, Sens. Actuators B 166–167 (2012) 117–127.
[12] Y. Oztekin, A. Ramanaviciene, A. Ramanavicius, Electrochemical determination of Cu(II) ions by 4-formylphenylboronic acid modified gold electrode, Electroanalysis 23 (2011) 1645–1653.
[13] Y. Oztekin, A. Ramanaviciene, N. Ryskevic, Z. Yazicigil, Z. Ustundag, A.O. Solak, A. Ramanavicius, 1,10-phenanthroline modified glassy carbon electrode for voltammetric determination of cadmium(II) ions, Sens. Actuators B 157 (2011) 146–153.
[14] Y. Oztekin, A. Ramanaviciene, A. Ramanavicius, Electrochemical copper (II) sensor based on self-assembled monolayer modified by 4-amino-6-hydroxy-2-mercaptopyrimidine monohydrate, Sens. Actuators B 155 (2011) 612–617.
[15] O. Breuer, U. Sundararaj, Nanocomposites based on conducting polymers and carbon nanotubes: from fancy materials to functional applications, J. Nanosci. Nanotechnol. 6 (2006) 289–302.
[16] C. Oueiny, S. Berlioz, F.X. Perrin, Carbon nanotube–polyaniline composites, Prog. Polym. Sci. 39 (2014) 707–748.
[17] J.D. Fowler, M.J. Allen, V.C. Tung, Y. Yang, R.B. Kaner, B.H. Weiller, Practical Chemical sensors from chemically derived graphene, ACS Nano 3 (2009) 301–306.
[18] H.J. Choi, In-yup Jeon, S.W. Kang, J.B. Baek, Electrochemical activity of a polyaniline/polyaniline-grafted multiwalled carbon nanotube mixture produced by a simple suspension polymerization, Electrochim. Acta 56 (2011) 10023–10031.
[19] C.J. Madadrang, H.Y. Kim, G. Gao, N. Wang, J. Zhu, H. Feng, M. Gorring, M.L. Kasnet, S. Hou, Adsorption behavior of EDTA-graphene oxide for Pb (II) removal, Appl. Mater. Interfaces 4 (2012) 1186–1193.
[20] J.H. Deng, X.R. Zhang, G.M. Zeng, J.L. Gong, Q.Y. Niu, J. Liang, Simultaneous removal of Cd(II) and ionic dyes from aqueous solution using magnetic graphene oxide nanocomposite as an adsorbent, Chem. Eng. J. 226 (2013) 189–200.
[21] Y. Oztekin, Z. Yazicigil, A. Ramanaviciene, A. Ramanavicius, Polyphenol-modified glassy carbon electrodes for copper detection, Sens. Actuatators B 152 (2011) 37–48.
[22] Y. Oztekin, Z. Yazicigil, A. Ramanaviciene, A. Ramanavicius, Square wave voltammetry based determination of copper (II) ions by polyluteolin- and polykaempferol-modified electrodes, Talanta 85 (2011) 1020–1027.
[23] Y. Oztekin, M. Tok, H. Nalvuran, S. Kiyak, T. Gover, Z. Yazicigil, A. Ramanaviciene, A. Ramanavicius, Electrochemical modification of glassy carbon electrode by poly-4-nitroaniline and its application for determination of copper (II), Electrochim. Acta 56 (2010) 387–395.
[24] J.P. Issi, L. Langer, J. Heremans, C.H. Olk, Electronic properties of carbon nanotubes: experimental results, Carbon 33 (1995) 941–948.
[25] Y.J. Zhang, Y.W. Lin, C.C. Chang, T.M. Wu, Conducting and magnetic behaviors of polyaniline coated multi-walled carbon nanotube composites containing monodispersed magnetite nanoparticles, Synth. Met. 16 (2011) 937–942.
[26] M.R. Mc Phail, J.A. Sells, Z. He, C.C. Chusuei, Charging nanowalls: adjusting the carbon nanotube isoelectric point via surface functionalization, J. Phys. Chem. C 113 (2009) 14102–14109.
[27] M.M. Musameh, M. Hickey, I.L. Kyratzis, Carbon nanotube-based extraction and electrochemical detection of heavy metals, Res. Chem. Intermed. 37 (2011) 675–689.
[28] E. Comini, Metal oxide nanowire chemical sensors: innovation and quality of life, Mater. Today 19 (2016) 559–567.
[29] Y. Zhu, S. Murali, W. Cai, X. Li, J.W. Suk, J.R. Potts, R.S. Ruoff, Graphene and graphene oxide: synthesis, properties, and applications, Adv. Mater. 22 (2010) 3906–3924.
[30] K.R. Ratinac, W. Yang, J.J. Gooding, P. Thordarson, F. Braet, Graphene and related materials in electrochemical sensing, Electroanalysis 23 (2011) 803–826.
[31] H. Huang, T. Chen, X. Liu, H. Ma, Ultrasensitive and simultaneous detection of heavy metal ions based on three-dimensional graphene-carbon nanotubes hybrid electrode materials, Anal. Chim. Acta 852 (2014) 45–54.
[32] E. Guo, Simultaneous electrochemical determination of lead and copper based on graphenated multi-walled carbon nanotubes, Int. J. Electrochem. Sci. 10 (2015) 7341–7348.
[33] Y. Wei, C. Gao, F.L. Meng, H.H. Li, L. Wang, J.H. Liu, X.J. Huang, SnO2/reduced graphene oxide nanocomposite for the simultaneous electrochemical detection of cadmium(II), lead(II), copper(II), and mercury(II): an interesting favorable mutual interference, J. Phys. Chem. C 116 (2012) 1034–1041.
[34] J. Zhang, L.B. Kong, B. Wang, Y.C. Luo, L. Kang, In-situ electrochemical polymerization of multi-walled carbon nanotube/polyaniline composite films for electrochemical supercapacitors, Synth. Met. 159 (2009) 260–266.
[35] L.M. Wierl, A.R. Guadalupe, H.D. Abruna, Multiple-use polymer-modified electrodes for electroanalysis of metal ions in solution, Anal. Chem. 57 (1985) 2009–2011.
[36] Y. Oztekin, Z. Yazicigil, A. Ramanavicieneb, A. Ramanavicius, Square wave voltammetry based on determination of copper (II) ions by polyluteolin- and polykaempferol-modified electrodes, Talanta 85 (2011) 1020–1027.
[37] L. Dedelaite, S. Kizilkaya, H. Incebay, H. Ciftci, M. Ersoz, Z. Yazicigil, Y. Oztekin,

A. Ramanaviciene, A. Ramanavicius, Electrochemical determination of Cu(II) ions using glassy carbon electrode modified by some nanomaterials and 3-nitroaniline, Colloids Surf. A 483 (2015) 279–284.
[38] F. De Riccardis, V. Martina, New method to obtain hybrid conducting nanocomposites based on polyaniline and carbon nanotubes, Energ. Ambiente Innov. 6 (2011) 86–95.
[39] I.Y. Jeon, H.J. Lee, Y.S. Choi, L.S. Tan, J.B. Baek, Semimetallic transport in nanocomposites derived from grafting of linear and hyperbranched poly(-phenylene sulfide)s onto the surface of functionalized multi-walled carbon nanotubes, Macromolecules 41 (2008) 7423–7432.
[40] O. Breuer, U. Sundararaj, Big returns from small fibers: a review of polymer/carbon nanotube composites, Polym. Compos 25 (2004) 630–645.
[41] L. Dai, A.W.H. Mau, Controlled synthesis and modification of carbon nanotubes and C60: carbon nanostructures for advanced polymeric composite materials, Adv. Mater. 213 (2001) 899–913.
[42] M. Kausala, C.Z. Liangchi, Fabrication and application of polymer composites comprising carbon nanotubes, Recent Pat. Nanotechnol. 1 (2007) 59–65.
[43] C. Oueiny, S. Berlioz, F.X. Perrin, Polyaniline–carbon nanotube composites, Pure Appl. Chem. 80 (2008) 2377–2395.
[44] H.L. Zhang, G.S. Lai, D.Y. Han, A.M. Yu, An amperometric hydrogen peroxide biosensor based on immobilization of horseradish peroxidase on an electrode modified with magnetic dextran microspheres, Anal. Bioanal. Chem. 390 (2008) 971–977.
[45] F.Y. Chuang, S.M. Yang, Titanium oxide and polyaniline core-shell nanocomposites, Synth. Met. 152 (2005) 361–364.
[46] M. Nagaraja, J. Pattar, N. Shashank, J. Manjanna, Y. Kamada, K. Rajanna, H.M. Mahesh, Electrical, structural and magnetic properties of polyaniline/pTSA-TiO2 nanocomposites, Synth. Met. 159 (2009) 718–722.
[47] Y. Yu, B. Che, Z. Si, L. Li, W. Chen, G. Xue, Carbon nanotube/polyaniline core-shell nanowires prepared by in situ inverse microemulsion, Synth. Met. 150 (2005) 271–277.
[48] A.K. Sharma, Y. Sharma, p-toluene sulfonic acid doped polyaniline carbon nanotube composites: synthesis via different routes and modified properties, J. Electrochem. Sci. Eng. 3 (2013) 47–56.
[49] J.L. Bantignies, J.L. Sauvajol, A. Rahmani, E. Flahaut, Infrared-active phonons in carbon nanotubes, Phys. Rev. B 74 (2006), 195425–5.